Framework Characterization of Mesostructured Carbon CMK-1 by X-ray Powder Diffraction and Electron Microscopy

Leonid A. Solovyov,*,† Vladimir I. Zaikovskii,‡ Alexandr N. Shmakov,‡ Oleg V. Belousov,† and Ryong Ryoo§

Institute of Chemistry and Chemical Technology, Krasnoyarsk 660049, Russia, Boreskov Institute of Catalysis, Novosibirsk 630090, Russia, and Department of Chemistry (School of Molecular Science-BK21), Korea Advanced Institute of Science and Technology, Taejon 305-701, Korea

Received: March 15, 2002

The model of structure and structural transformation of the mesostructured carbon material CMK-1 was established by X-ray powder diffraction (XRD) and transmission electron microscopy (TEM) investigations. The investigations showed that the enantiomeric carbon subframeworks formed within the pores of the MCM-48 mesoporous template used for the material synthesis displaced with respect to one another without significant distortions after the dissolution of the silica wall of the template. The model proposed agrees well with TEM images observed. The XRD structural modeling of CMK-1 done using the continuous density function technique allowed perfect fit of the calculated to the experimental powder diffraction pattern and provided geometric characteristics of the material texture. The structural characteristics obtained agreed fairly well with TEM analysis and with previously reported adsorption data.

Introduction

Resently, a series of mesostructured carbon materials designated as CMK-1,2,3,4,5[1−8] and SNU-1,2[9,10] have been synthesized using ordered silicate mesoporous templates.[11−14] The physicochemical properties of mesostructured carbons, such as large pore volume, high specific surface area, chemical inertness, and solidity together with the ordered mesopore structure make them quite promising in many applications, including catalysis, adsorption of bulky molecules, chromatography, hydrogen storage, and manufacturing of electrode materials. Some materials from the above series have already been shown to exhibit attractive electrochemical double-layer capacitance behavior.[9,10,15] The material CMK-1 supporting Pt and Pd clusters was demonstrated to have advanced catalytical performance in terms of conversion and selectivity for liquid-phase hydrogenation reactions of nitrobenzene, 2-ethylanthraquinone, and 4-isobutylacetophenone, compared with commercial carbon-supported precious metal catalysts.[16]

The templating synthesis approach used for fabricating the mesostructured carbons consisted in impregnation of a carbon source substance into the mesopores of the template followed by thermal carbonization and dissolution of the silica wall.[1−10] The resulted mesostructure depended on the type of the template used. The materials CMK-2,3 and 4 were shown[4−7] to be negative replicas of the mesoporous silica templates SBA-1,[17] SBA-15,[18] and MCM-48,[11] respectively. In contrast, the structure of CMK-1 and SNU-1 materials, synthesized using silicate and aluminosilicate MCM-48 templates, was found to be not the exact negative replica of the template. This was ascribed to a transformation of the mesostructure after the dissolution of the template wall. The main indication of the structural transformation was the appearance on the X-ray diffraction (XRD) powder patterns of CMK-1 and SNU-1 of a strong low-angle diffraction peak that was not consistent with the symmetry of MCM-48.[1,9]

In the current study, the model of structure and structural transformation of the carbon molecular sieve CMK-1 is proposed based on XRD and TEM data. The textural and geometric characteristics of the CMK-1 material determined by the XRD structural modeling are compared with those previously reported obtained by the nitrogen adsorption analysis.[2]

Experimental Section

The material CMK-1 was prepared using MCM-48 template by a recently reported procedure involving impregnation with sucrose in the presence of sulfuric acid, followed by carbonization and removal of the silica template in NaOH solution.[1]

TEM images were obtained in the bright field mode on a JEM 2010 electron microscope having 0.14 nm instrumental resolution. X-ray powder diffraction data were collected on a high-resolution diffractometer located in Siberian Center of Synchrotron Radiation. The Ge(111) plane perfect crystal analyzer on the diffracted beam ($\lambda = 0.15405$ nm) along with high natural collimation of the synchrotron beam provide high instrumental resolution of the diffractometer. The instrumental half-width of the XRD reflections is about 0.04° in the low-angle region of $1-7°$ 2θ. Vertical parallel Soller's collimator with a 5 mrad divergence was applied to restrict azimuth divergence of the diffracted beam and to reduce the low-angle peak asymmetry.

The XRD structural modeling was done using the continuous density function technique[19] and the Rietveld's full-profile formalism.[20] On the basis of the diffraction peak positions, the cubic unit cell parameter a_0 of the CMK-1 material was determined to be 8.36(1) nm. To build the model function $\rho(r)$, simulating the density distribution in the material the nodal approximation[21] of the triply periodic minimal "Gyroid" (G)

* To whom correspondence should be addressed. E-mail: leosol@icct.ruo. Phone: +7-3912-495-663. Fax: +7-3912-238-658.
† Institute of Chemistry and Chemical Technology.
‡ Boreskov Institute of Catalysis.
§ Korea Advanced Institute of Science and Technology.

10.1021/jp0257653 CCC: $22.00
Published on Web 11/05/2002

surface[22] was used. It is known that the silica wall in MCM-48 goes parallel to the G surface.[23] Recently, it has been shown that the G surface could be closely approximated by the following nodal surface[21]

$$G(r) = \sin X \cos Y + \sin Y \cos Z + \sin Z \cos X = 0 \quad (1)$$

where $X = 2\pi x$, $Y = 2\pi y$ and $Z = 2\pi z$. Using eq 1, we constructed a function that allows simulating the density distribution in MCM-48 and related Gyroid-like mesostructures:

$$\rho(\mathbf{r}) = \begin{cases} \rho_1 \text{ for } G(\mathbf{r}-\mathbf{v}) < -L, \\ \rho_2 \text{ for } G(\mathbf{r}+\mathbf{v}) > L, \\ \rho_0 \text{ for } G(\mathbf{r}-\mathbf{v}) \geq -L \text{ and } G(\mathbf{r}+\mathbf{v}) \leq L \end{cases} \quad (2a)$$

$$L = \frac{\sqrt{3}}{2} \sin \frac{2\pi h_w}{\sqrt{3} a_0} \quad (2b)$$

where $\rho_0 \cdots \rho_2$ are the values of density in different regions of the material, v is the displacement vector of the regions, h_w is the flatwise distance between the surfaces bounding the region ρ_0 with no displacement, and a_0 is the cubic unit cell parameter. On $v = 0$ this function simulates the matter distribution with constant density ρ_0 in the vicinity of thickness h_w around the G surface and with densities ρ_1 and ρ_2 within the right and left-handed enantiomeric volumes separated by the ρ_0 zone. For a calcined MCM-48 material with empty pores the values of ρ_1, ρ_2, and v are zero. In this case, the function $\rho(r)$ simulates the density distribution in MCM-48 with the wall of nearly constant thickness h_w and density ρ_0. In general, this function allows the density distribution simulation for different composite and framework materials with structural elements following the G surface topology.

To check the applicability of the model developed to Gyroid mesostructures, we made preliminary fitting of the XRD powder pattern of MCM-48 sample using the simulative density function $\rho(r)$. The result of fitting is shown in Figure 1a. The refined parameters were the unit cell dimension $a_0 = 9.601$ nm, wall thickness $h_w = 0.98$ nm, and the Debye−Waller factor. The remaining parameters were constrained as follows: $\rho_1 = \rho_2 = 0$ and $\rho_0 =$ constant. As seen from the figure, the experimental and calculated XRD powder patterns for MCM-48 after the refinement demonstrate good consistency.

Results and Discussion

In MCM-48, pores form two enantiomeric bicontinuous branched self-intersecting volumes separated by an infinite wall following the G surface. The carbon material formed inside this pore system is expected to consist of two separate enantiomeric subframeworks. A fragment of one subframework is shown in Figure 1b. It may be considered as built of conjugate trefoil fragments formed by roughly cylindrical segments. The extended structure presents interwoven ring-frames as shown in Figure 2. Such structure does not permit an uncoupling of the carbon subframeworks after the dissolution of the silica wall, unless the particles of the material are too small (or thin) or the frameworks are partly broken. The TEM analysis revealed the presence of some amount of the individual uncoupled subframeworks in the material (Figure 3), but this amount was minor.

The XRD powder pattern of the CMK-1 material (Figure 1c) demonstrates narrow diffraction peaks with half-width of about 0.1° 2θ, which allow characterization of the material as highly ordered. Although the angular range of the observed reflections

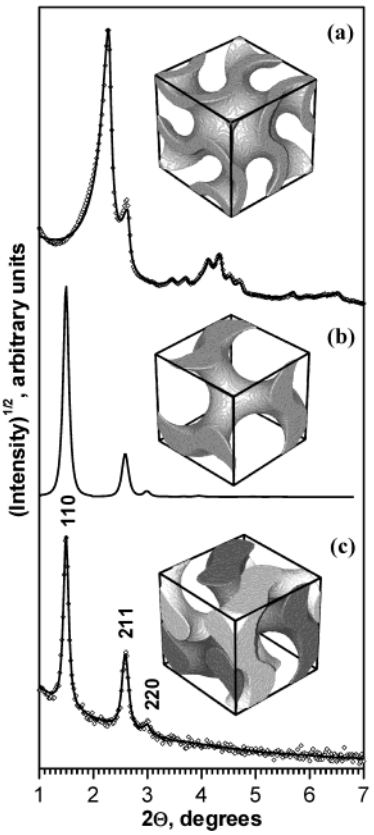

Figure 1. Models of the structure unit cell and XRD powder patterns (root-square weighted) for the MCM-48 material (a), a single enantiomeric carbon sub-framework (b), and the CMK-1 material (c). The experimental profiles are shown by diamonds and calculated by solid line.

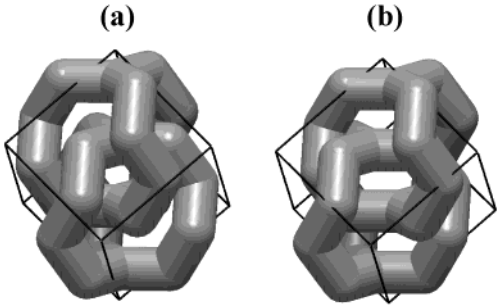

Figure 2. Fragments of the interwoven carbon framework structure in the model of undisplaced (a) and displaced along ⟨110⟩ (b) enantiomeric subframeworks. The unit cell is depicted by lines.

is not enough for an explicit separation of size- and strain-induced broadening of the diffraction peaks, it is though possible to make a plausible estimation. The low limit of the mean coherent domain size of the material may be estimated from the width of the first (low angle) observed diffraction peak after the separation of the instrumental broadening, assuming zero strain-broadening. For the investigated material, such estimation gives the value of about 100 nm, which means that the bulk of the material consists of ordered arrays with dimensions greater than 100 nm. The framework dimensions of 100 nm and greater do not, evidently, permit an uncoupling of the carbon subframeworks.

The structural transformation of the interwoven carbon framework after the dissolution of the silica wall may be expected to consist of two stages. The subframeworks may be displaced with respect to one another to form contacts. Further transformation may as well involve a distortion of the frame-

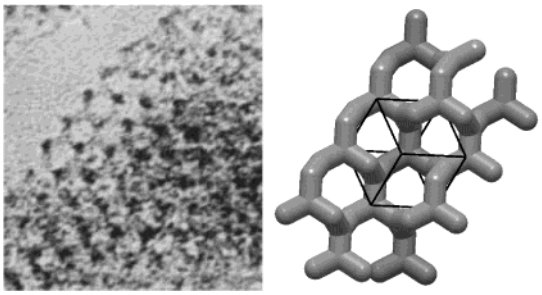

Figure 3. TEM image of CMK-1 demonstrating a fragment of single uncoupled carbon subframework (left) and respective structure model (right).

works. The simple displacement of the frameworks without distortion does not require any additional energy, and therefore, this kind of transformation is the easiest and the most feasible one. On the contrary, the distortion of the frameworks implies the existence of strong interactions between their surfaces, which is unlikely for the already formed carbon material. An earlier study showed that after the silica wall dissolution the unit cell parameter of the material remained practically unchanged.[2] This gives an additional argument for excluding the framework distortion from the structure model, because any framework deformation must have inevitably induced a transformation of the unit cell. Below, it will be shown that the model of the undistorted framework displacement is all-sufficient and fully consistent with available TEM, XRD, and adsorption data.

The main fact pointing to the structure transformation of the material is the appearance of a strong low-angle diffraction peak in the XRD powder pattern that is not consistent with the space group $Ia\bar{3}d$ of the MCM-48 template. This reflection is indexed as 110, and its emergence may be explained by lowering the material symmetry. In the low-angle area, the reflection 110 is, in fact, the only one allowed by the space group I_132 characterizing the symmetry of single enantiomeric subframework. The XRD powder pattern simulation (Figure 1b) done with the help of the model function $\rho(r)$ shows that the 110 reflection from single carbon subframework is fairly strong. Its relative intensity is about 2−3 times higher than that observed for the CMK-1 material. The calculations for the model of two undistorted but displaced enantiomeric subframeworks show that such a model also gives strong 110 reflection and, furthermore, it provides full consistency between the observed and calculated XRD powder patterns of CMK-1, as shown in Figure 1c.

As the displacement of the subframeworks is supposed to have no relation to any certain interaction between their surfaces, then one may expect a random direction of shift in different parts and particles of the material. However, among different possible framework junctions that can be formed after the displacement, the most stable configurations must, presumably, have the least degree of freedom. By analyzing different displaced framework configurations, we concluded that the least degree of freedom might be provided by the shift of the subframeworks along the ⟨110⟩ directions (Figure 2b). Consequent TEM analysis also showed that the shift in this direction best explained the observed images.

The symmetry of the material with displaced subframeworks is lower than the symmetry $Ia\bar{3}d$ of MCM-48 template. The framework shift along the ⟨110⟩ direction excludes all of the symmetry elements of the structure except one 2-fold axis oriented along ⟨110⟩ and the inverse center. The symmetry of such a configuration can be characterized by the monoclinic space group $C2/c$. An arbitrary framework shift preserves only

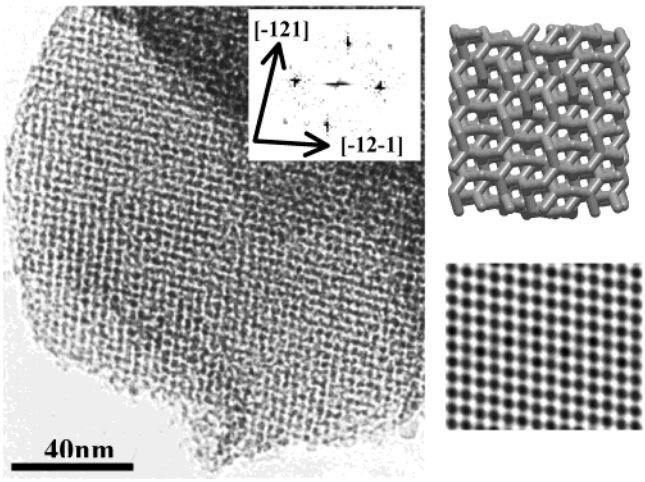

Figure 4. TEM image of CMK-1 viewed from the [531] direction (left) with respective structure model and TEM image simulation (right).

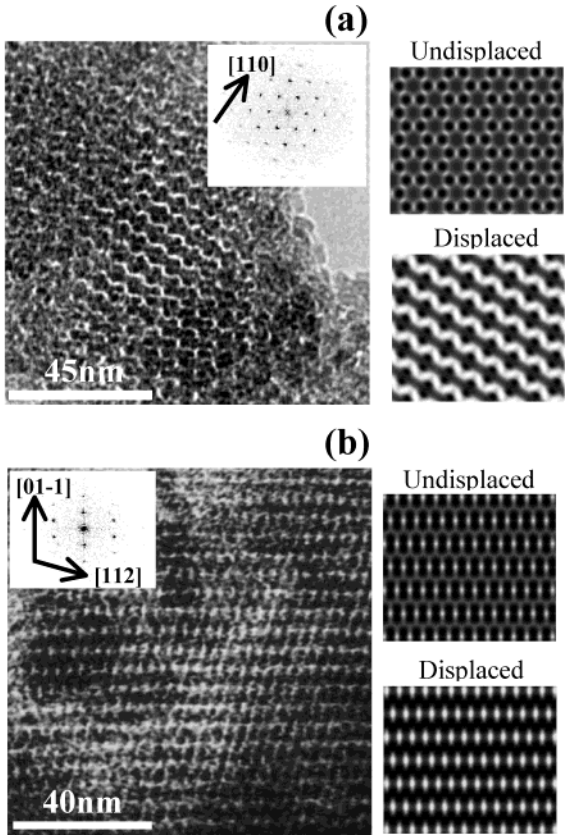

Figure 5. TEM images (left) of CMK-1 viewed from the [111] (a) and [−311] (b) directions and respective TEM image simulations (right) based on the models of undisplaced and displaced sub-frameworks.

the inverse center, thus decreasing the symmetry to the triclinic space group $P\bar{1}$ or, if to stick to the former cubic translation vectors, $I\bar{1}$. For convenience, we shall use the space group $I\bar{1}$ in further consideration of the CMK-1 structure, which facilitates the comparison of the structural parameters of CMK-1, MCM-48, and the silica/carbon composite.

The proposed structure model of the displaced frameworks explicitly explains observed TEM images of the CMK-1 material. In Figures 4 and 5, some representative TEM images of the material are shown compared with those simulated on the basis of the structure model proposed. The image simulation was done by projecting the density distribution $\rho(r)$ calculated

for respective structure model. Figure 4 shows a particle of the material viewed from the [531] direction that is the intersection of planes (−121) and (−12−1). As seen, respective structure projection and TEM image simulation correspond quite well with the observed pattern. In Figure 5a, a fragment of the material is observed viewed from the [111] direction. A similar fragment was also presented for CMK-1 in an earlier publication.[4] The pattern observed is not consistent with the cubic symmetry, because the 3-fold axis here is absent. As seen from Figure 5a, this pattern does not agree as well with the structure model of undisplaced frameworks, but it fully agrees with the model of the framework displaced along the ⟨110⟩ direction. The TEM image for the [−311] projection shown in Figure 5b also allows fair matching between the observed pattern and the TEM image simulation based on the proposed structure of CMK-1.

The XRD structural modeling of CMK-1 was done using the simulative density distribution function $\rho(r)$. The set of diffraction reflections was generated in accordance with the $I\bar{1}$ space group. The varying parameters were h_w and υ, with $\rho_0 = 0$ and $\rho_1 = \rho_2 =$ constant. The components υ_x and υ_y of υ were constrained to be equal, and υ_z was assigned a value of zero in order to simulate the framework displacement along [110] direction. The Debye−Waller factor was applied to allow for the disordering and surface roughness of the carbon frameworks. The best fit to the experimental XRD powder pattern (Figure 1c) was obtained with $h_w = 1.3(1)$ nm and $\upsilon_x = \upsilon_y = 0.06(1)$.

According to the definition of $\rho(r)$ by eq 2, the term h_w for CMK-1 material should be interpreted as a mean flatwise distance between the surfaces of the carbon frameworks before the dissolution of the silica wall (i.e., in the carbon/silica composite). The obtained value of h_w is somewhat higher than the wall thickness of the MCM-48 template (ca. 1 nm) determined by the adsorption analysis.[2] This may be explained both by the existence of a gap between the silica wall and the carbon material and by the silica wall thickening after the high-temperature treatment as it was proposed earlier.[2] The obtained magnitude of υ_x and υ_y correspond to the total mutual displacement of the subframeworks at 1.4(2) nm. This value coincides with h_w within standard deviations, which is consistent with the proposed structure model, as the subframeworks indeed must shift at the distance between their surfaces.

Using the experimental reflection intensities extracted from the XRD powder profile, we calculated the electron density distribution Fourier-map for the CMK-1 material. The intensities were extracted from the profile with the LeBail algorithm.[24] The initial phases required for the calculation were derived basing on the fitted simulative function $\rho(r)$. In Figure 6, some sections of the Fourier-map for the CMK-1 are shown in comparison with the respective sections for MCM-48. As seen, the sections of the CMK-1 maps clearly demonstrate displaced contiguous frameworks following the shape of the MCM-48 mesopores.

The framework structure of CMK-1 is too complex to be described in such simple terms as "pore", "wall", or "diameter" commonly used for describing the texture of mesoporous materials and molecular sieves. Nevertheless, it would be expedient to make an estimation of its geometric characteristics. The diameter of the roughly cylindrical framework segments may be determined using the obtained value of h_w. The centers of these segments coincide with the Wyckoff symmetry positions 12c and 12d of the $I4_132$ space group. The distance between these positions equals the half of the cubic unit cell parameter. Hence, the diameter d_s of the framework segments

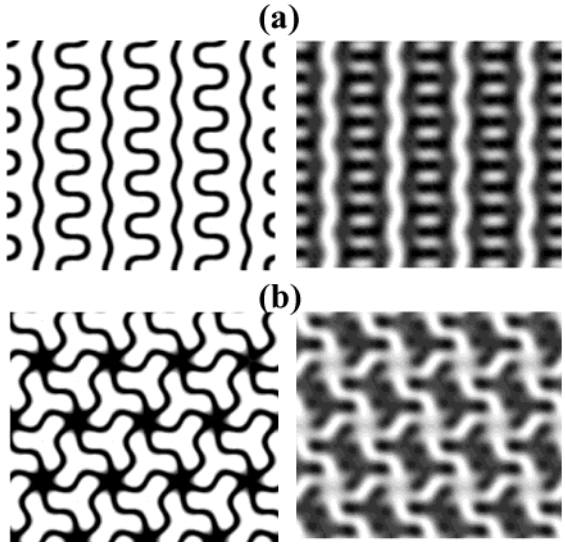

Figure 6. Characteristic sections (211) (a) and (111) (b) of the electron density distribution Fourier-map for the MCM-48 (left) and the CMK-1 materials (right).

of CMK-1 material may be calculated as

$$d_s = \frac{a_0}{2} - h_w \qquad (3)$$

or, for the material under study, $d_s = 2.9(1)$ nm. This value is noticeably lower than the mean pore diameter of the MCM-48 template (ca. 4 nm), which can be explained by the structure shrinkage and possible wall thickening after the high-temperature treatment of the carbon/silica composite as proposed earlier.[2] The above estimation of d_s agrees well with the dimensions of the sub-framework observed on the TEM image shown in Figure 3.

The utmost flatwise distance between the carbon framework surfaces can be estimated by the summation of h_w and the framework mutual displacement, which gives the value of 2.7(2) nm. In a recent study,[2] the adsorption-based mesopore diameter of CMK-1 was evaluated at 2.9 nm using the DFT Plus software developed for carbons with slitlike pore geometry.[25] As seen, the above values obtained by two different methods are quite comparable, whereas the pore system of CMK-1 is complex and requires a special model for its adsorption textural characterization. This complexity of the CMK-1 pore system with broad dispersion of the characteristic intersurface distances between the displaced carbon frameworks may as well explain the relative flatness of the capillary condensation step on nitrogen adsorption isotherms for CMK-1 compared to those for MCM-48.[2]

Conclusions

The current study showed that the structure of the mesostructured carbon material CMK-1 could be described as the ordered interwoven assembly of two enantiomeric subframeworks reproducing the shape of the MCM-48 mesopores. The subframeworks are displaced with respect to one another to form contacts without significant distortions. The minor part of the material presents uncoupled individual subframeworks. The XRD structural modeling using the continuous density function technique allowed determination of the geometric textural characteristics of the material, such as the framework thickness and the interframework displacement distance. The structure characteristics obtained are consistent with both TEM observa-

tions and the previously reported adsorption data. The results of the investigations provide a basis for the quantitative structural analysis of other derivative and composite mesostructured materials synthesized using MCM-48 as the template.

Acknowledgment. This work is supported by INTAS Fellowship grant for Young Scientists YSF 2001/2-3, INTAS grant 01-2283, and joint Grant KRSF-RFBR 02-03-97704.

References and Notes

(1) Ryoo, R.; Joo, S. H.; Jun, S. *J. Phys. Chem. B* **1999**, *103*, 7743.

(2) Kruk, M.; Jaroniec, M.; Ryoo, R.; Joo, S. H. *J. Phys. Chem. B* **2000**, *104*, 7960.

(3) Joo, S. H.; Jun, S.; Ryoo, R. *Microporous Mesoporous Mater.* **2001**, *44*−*45*, 153.

(4) Ryoo, R.; Joo, S. H.; Kruk, M.; Jaroniec, M. *Adv. Mater.* **2001**, *13*, 677.

(5) Jun, S.; Joo, S. H.; Ryoo, R.; Kruk, M.; Jaroniec, M.; Liu, Z.; Ohsuna, T.; Terasaki, O. *J. Am. Chem. Soc.* **2000**, *122*, 10712.

(6) Shin, H. J.; Ryoo, R.; Kruk, M.; Jaroniec, M. *Chem. Commun.* **2001**, 349.

(7) Ryoo, R.; Joo, S. H.; Jun, S.; Tsubakiyama, T.; Terasaki, O. *Stud. Surf. Sci. Catal.* **2001**, *135*, 150.

(8) Joo, S. H.; Choi, S. J.; Oh, I.; Kwak, J.; Liu, Z.; Terasaki, O.; Ryoo, R. *Nature* **2001**, *412*, 169.

(9) Lee, J.; Yoon, S.; Hyeon, T.; Oh, S. M.; Kim, K. B. *Chem. Commun.* **1999**, 2177.

(10) Lee, J.; Yoon, S.; Oh, S. M.; Shin, C.; Hyeon, T. *Adv. Mater.* **2000**, *12*, 359.

(11) Beck, J. S.; Vartuli, J. C.; Roth, W. J.; Leonowicz, M. E.; Kresge, C. T.; Schmitt, K. D.; Chu, C. T.-W.; Olson, D. H.; Sheppard, E. W.; McCullen, S. B.; Higgins, J. B.; Schlenker, J. L. *J. Am. Chem. Soc.* **1992**, *114*, 10834.

(12) Kresge, C. T.; Leonowicz, M. E.; Roth, W. J.; Vartuli, J. C.; Beck, J. S. *Nature* **1992**, *359* 710.

(13) Corma, A. *Chem. Rev.* **1997**, *97*, 2373.

(14) Ciesla, U.; Schuth, F. *Microporous Mesoporous Mater.* **1999**, *27*, 131.

(15) Yoon, S.; Lee, J.; Hyeon, T.; Oh, S. M. *J. Electrochem. Soc.* **2000**, *147*, 250.

(16) Ahn, W. S.; Min, K. I.; Chung, Y. M.; Rhee, J. K.; Joo S. H.; Ryoo, R. *Stud. Surf. Sci. Catal.* **2001**, *135*, 313.

(17) Huo, Q.; Leon, R.; Petroff, P. M.; Stucky, G. D. *Science* **1995**, *268*, 1324.

(18) Zhao, D.; Feng, J.; Huo, Q.; Melosh, N.; Fredirckson, G. H.; Chemlka, B. F.; Stucky, G. D. *Science* **1998**, *279*, 548.

(19) Solovyov, L. A.; Kirik, S. D.; Shmakov, A. N.; Romannikov *Microporous Mesoporous Mater.* **2001**, *44*−*45*, 17.

(20) Rietveld, H. M. *J. Appl. Crystallogr.* **1969**, *2*, 65.

(21) Gandy, P. J. F.; Bardham, S.; Mackay, A. M.; Klinowski, J. *Chem. Phys. Lett.* **2001**, *333*, 427.

(22) Schoen, A. H. *NASA Technical Note D-5541*; NASA: Washington, DC, 1970.

(23) Monnier, A.; Schuth, F.; Huo, Q.; Kumar, D.; Margolese, D.; Maxwell, R. S.; Stucky, G. D.; Krishnamurty, M.; Petroff, P.; Firouzi, A.; Janicke, M.; Chmelka, B. F. *Science* **1993**, *261*, 1299.

(24) Le Bail, A.; Duroy, H.; Fourquet, J. L. *Mater. Res. Bull.* **1988**, *23*, 447.

(25) Olivier, J. P. *Carbon* **1998**, *36*, 1469.